Journal of Engineering Physics and Thermophysics, Vol. 76, No. 6, 2003

NEW METHODS OF LASER ANEMOMETRY IN INVESTIGATIONS OF COMBINED GASDYNAMIC FLOWS

Yu. N. Dubnishchev,[a] B. S. Rinkevichius,[b] and N. A. Fomin[c]

UDC 533.6.08+533.6.011.8

New developments in laser anemometry which are based on digital technologies of input and processing of images using CCD chambers and personal computers are analyzed. The capabilities of digital dynamic speckle photography are illustrated by the intensity fields obtained for surface blood flow in biotissues. Two-phase flows are investigated with the use of a new PIV technique. New developments in the field of laser anemometry which are based on the use of coherent optical Doppler processors and enable us to pass from the local diagnostics to the diagnostics of two-dimensional fields of velocity and its visualization are described.

Introduction. Over a long period of time, laser-anemometry methods in investigation of gasdynamic flows have been confined to the use of laser Doppler anemometers based on recording of the Doppler shift of the frequency of laser radiation which is scattered by visualizing particles specially added to the flow under study and moving with the medium *in a separated microvolume* [1]. At the same time, multiple attempts at directly photographing visualizing particles *in a separated plane* to simultaneously determine the two-dimensional field of velocity of flow had been made even before the appearance of lasers [2]. At a later time, this technique received the name "track method." (In the English-language scientific literature, this method was called "tracer photography." The term "PTV" (Particle Tracking Velocimetry) is used as present.) The use of laser illumination in analogous experiments ("laser-knife method") and the progress made in coherent optical processing of the images obtained ("Young method of interference fringes") led to a both a significant improvement in the accuracy of processing of the images obtained and the possibility of accumulating large arrays of experimental information with its automated processing (both are necessary for construction of two-dimensional fields of velocities of the flows under study with a high spatial resolution). In the first publications on the new laser anemometry based on the coherent techniques of processing of images, the methods used were called "speckle anemometry in scattered light" and "speckle photography" [3–5]. At a later time, these methods received the name PIV. (The term "PIV," an acronym for "Particle Image Velocimetry," is widely used now not only in the English-language literature but also in the French, German, Japanese, and other languages. The translation of the term into the Russian language has no convenient acronym; therefore, it is proposed that the term "PIV" be also used in the Russian language by analogy with others in word combinations of the type "PIV methods," "PIV technique", etc. This will continue the tradition of using the agreed-upon term *speckle* in Russian (just as in other languages) in word combinations of the type *speckle photography*, *speckle interferometry*, *speckle technique*, etc. We note that this terminology also differs from that initially proposed in the Russian literature — *interferometry in diffuse light*, see [6]. Particle image velocimetry (particle image anemometry) is a currently widespread and rapidly developing method of measurement of the velocity fields of particles in liquid and gas flows (see [7–12]). The complete PIV bibliography encompasses several thousands titles today. The present paper seeks to describe results of development of the PIV technique at the Institute of Thermal Physics of the Siberian Branch of the Russian Academy of Sciences, the Moscow Power Institute (Technical University), and the Heat and Mass Transfer Institute of the National Academy of Sciences of Be-

[a]Institute of Thermal Physics, Siberian Branch of the Russian Academy of Sciences, Novosibirsk, Russia; [b]Moscow Power Institute (Technical University), Moscow, Russia; [c]A. V. Luikov Heat and Mass Transfer Institute, National Academy of Sciences of Belarus, 15 P. Brovka Str., Minsk, 220072, Belarus; email: fomin@hmti.ac.by. Translated from Inzhenerno-Fizicheskii Zhurnal, Vol. 76, No. 6, pp. 3–12, November–December, 2003. Original article submitted May 22, 2003.

1062-0125/03/7606-1197$25.00

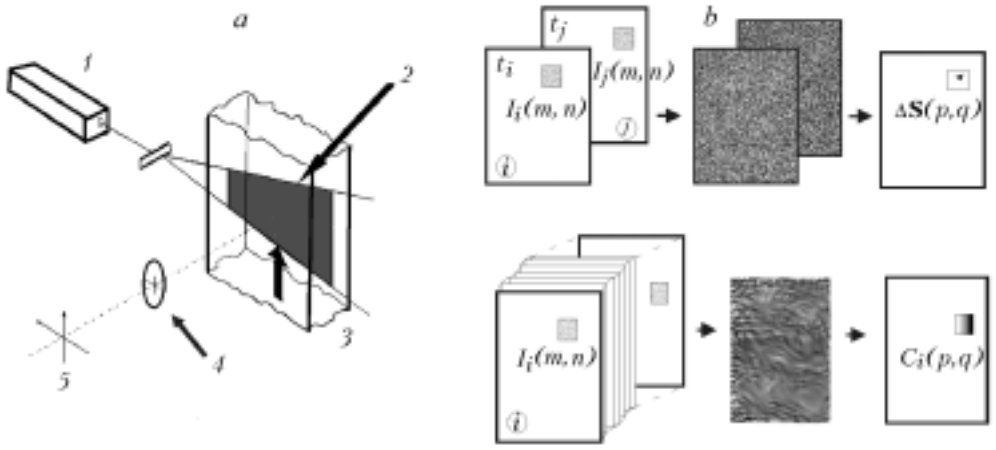

Fig. 1. Geometry of illumination in the "standard" PIV technique (a) [1) laser; 2) "laser knife"; 3) flow under study; 4) representing lens; 5) image plane] and basic methods of processing of PIV pictures (speckle fields) (b).

larus (these results have been obtained in carrying out the INTAS project "Novel PIV Systems in Fluid Mechanics Measurements"[*)].

Basic Principles of the PIV Technique. The "standard" PIV technique is based on an analysis of the displacement of the images of particles visualizing the flow under study in a time interval between successive frames in filming of these particles in a separated region, as is shown in Fig. 1. The visualizing particles are assumed to be uniformly introduced into the flow under study. The particles must be fairly small for the particle velocities to completely "track" the flow. These are usually particles of micron or even submicron size, just as in Doppler meters [10].

Laser radiation scattered by the particles is recorded with high-resolution photographic plates or by digital CCD chambers (CCD — charge-coupled device). Depending on the number of particles in a unit volume in the image plane this radiation forms either the images of individual particles or a speckle field. The particle displacement sought is determined by a cross-correlation analysis of two successive images. For this purpose the obtained image of the speckle field is broken into small subregions in each of which we compute the cross-correlation function in relation to the coordinates of the CCD chamber (m, n):

$$R_{ij}(p, q) = \frac{MN}{(M-p)(N-q)} \left[\frac{\sum_{m=1}^{M-p} \sum_{n=1}^{N-q} I_i(m, n)\, I_j(m+p, n+q)}{\sum_{m=1}^{M} \sum_{n=1}^{N} I_i(m, n)\, I_j(m, n)} \right]. \quad (1)$$

This function has a maximum for $p = p^*$ and $q = q^*$. It is the coordinates p^* and q^* that determine the average-over-the-subregion displacement of particles in the values of the cell size d^*. Thus, the modulus of the displacement vector can be computed from the relation $|\mathbf{\Delta d}| = d^* \sqrt{(p^*)^2 + (q^*)^2}\, \mathfrak{M} = d^* |\mathbf{\Delta}| \mathfrak{M}$, where $\mathfrak{M}$ is the coefficient of optical magnification of an image-forming optical system from a visualizing particle to a CCD matrix. The particle-image displacement $|\mathbf{\Delta^2}| = \sqrt{(p^*)^2 + (q^*)^2}$ is determined with a very high degree of accuracy. The error of such determination can amount to units of a percent of the CCD-cell size d^* due to the overdetermination of the system and the statistical character of computations from relation (1).

In investigating comparatively slow processes, in which we are able to "fix" the particle distribution in the image plane during a "short" exposure, we record the time order of images (speckle fields) and make a cross-correla-

[*)] INTAS project 00-0135 "Novel PIV Systems in Fluid Mechanics Measurements," project supervisor Dr. Jürgen Kompenhans (Germany).

tion analysis of the images corresponding to different instants of time t_1, t_2, ..., t_n. Computing the coordinates of the maximum of the cross-correlation function $R_{ij} = \langle I_i I_j \rangle / \langle I_i \rangle \langle I_j \rangle$, we determine the velocity vector sought in the subregion that is characterized by the indices (p, q) from the relation

$$\mathbf{V}(p, q) = \frac{\Delta \mathbf{d}(p, q)}{t_j - t_i}.$$

For superfast processes when the image of particles is "blurred" even during a "short" time interval, in analyzing the specklograms obtained we use an autocorrelation analysis enabling us to determine the contrast of the speckle field:

$$C_i = \frac{\sigma_{I_i}}{\langle I_i \rangle} = \frac{\sqrt{\langle I_i \rangle^2 - \langle I_i^2 \rangle}}{\langle I_i \rangle} = \sqrt{\left[\frac{1}{MN} \sum_{m=1}^{M} \sum_{n=1}^{N} I_i \right]^2 - \frac{1}{MN} \sum_{m=1}^{M} \sum_{n=1}^{N} I_i^2} \Big/ \frac{1}{MN} \sum_{m=1}^{M} \sum_{n=1}^{N} I_i . \quad (2)$$

The value of this contrast is dissimilar in different subregions of the specklegram and turns out to be in inverse proportion to the velocity of particles at the corresponding point of flow at the instant of exposure. It has been shown that from the value of this contrast one can determine the velocity of both a rough solid body illuminated by laser radiation [13] and a diffuse body in which the scattering particles move with dissimilar velocities at different points of space. Living biotissues the laser radiation in which is scattered by moving erythrocytes have been examples of such diffuse bodies [14].

Development of the PIV Technique. The "standard" PIV technique enables us to obtain the two-dimensional field of projections of the particle-velocity vector onto the image plane: $\mathbf{V} = \mathbf{V}(x, y) = V_x \cdot \mathbf{i} + V_y \cdot \mathbf{j}$ in both the laminar and turbulent flows [15, 16]. To determine the third velocity component we must obtain two (or several) two-dimensional projections and display the two-dimensional vector field $\mathbf{V} = V_x \cdot \mathbf{i} + V_y \cdot \mathbf{j} + V_z \cdot \mathbf{k}$ sought, employing simple geometric constructions. Such a PIV method is called stereoscopic [17]. Special chambers enabling one to simultaneously record the projections of particle displacement onto different planes have been constructed at present for obtaining such information. Different scanning systems have been developed [18] and the capabilities of holography [19] and of the new three-dimensional laser Doppler anemometers [20] employing coherent optical processors of PIV pictures have been investigated for obtaining three-dimensional velocity distributions (see below).

PIV Measurements in Real Time. The development of digital technologies for putting images into a personal computer with the use of CCD chambers in combination with the progress made in cross-correlation analysis of PIV pictures and speckle fields has opened up fresh opportunities for diagnostics of gasdynamic flows on the basis of a digital PIV technique (DPIV) (see [10]). In the case of the employment of a "classical" photographic technique one carries out "instantaneous" recording of the particle distribution in the flow at two different instants of time on one negative, development of the negative, and subsequent optical analysis of the specklegram obtained with the aim of determining the average displacement of particles in each small (corresponding to a certain small region of flow) subregion ("subzone") of the negative. Finally, one determines the vector of flow velocity at each "subzone," whose number can be very large ($\sim 10^6$ or more, see [11]). It is precisely this fact — the possibility of obtaining vast arrays of experimental information — that has determined the considerable progress made by the PIV technique in investigating combined turbulent flows whose analysis and description are possible only with statistical methods.

The evident drawback of photographic systems is that the negative is subjected to photographic development, which requires special conditions and time. The situation is fundamentally different in digital recording of speckle fields. In this case, the optical processing of a specklegram can also be replaced by its numerical cross-correlation analysis enabling one to determine the same parameter — the vector of the average displacement of speckles in each separated subzone of the speckleogram stored in the personal computer. When the "standard" CCD chambers with the number of cells $\sim 1000 \times 1000$ is employed, the dimension of the "subzones" can be $\sim 32 \times 32$, $\sim 64 \times 64$, or even $\sim 128 \times 128$. The number of elementary cells in each "subzone" remains sufficient for statistical averaging in computation of the cross-correlation function. Such computations on modern personal computers can be performed in a time interval between successive frames in recording digital images in TV standard (this interval is 40 μsec at a frequency of 25 Hz), which makes it possible to construct diagnostic systems in real time.

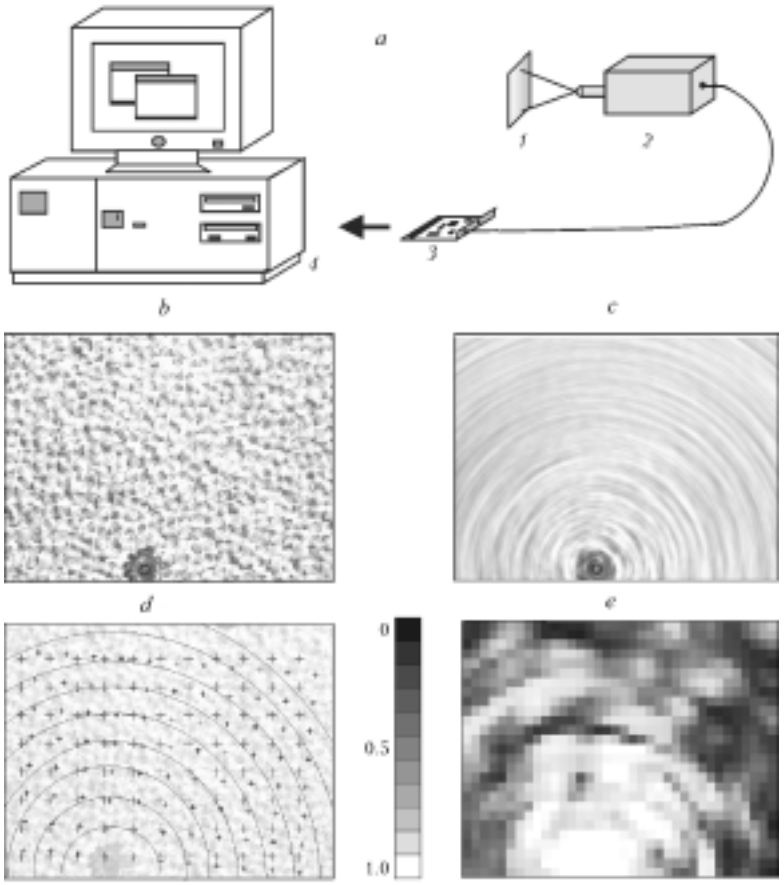

Fig. 2. Block diagram of the setup for digital speckle photography of fast processes (a) [1) speckle field; 2) IMASYS CCD chamber; 3) analog-to-digital converter of the videosignal (16 bits) + graphic map (2 Mb); 4) personal computer]; b–e) examples of experimental results on investigation of a rotating disk (form of the rotating disk and results of data processing by cross-correlation and autocorrelation analysis); crosses in d, average displacement of the speckles over the period between exposures, curves, isolines of these displacements.

In the present work, we have realized a program of processing of images in "quasireal" time the computation and analysis of the cross-correlation function (1) according to which takes ~300 μsec on a medium-class personal computer (Pentium, 133 MHz). The frequency of outputting the data processed to a monitor is about 1–2 Hz, which is sufficient for direct visualization of comparatively low-frequency processes, for example, laminar flames or spatial and temporal changes in the surface bloodflow *in vivo* [14]. A block diagram of the system of digital recording of speckle fields at the Heat and Mass Transfer Institute is shown in Fig. 2a. The speckle field was generated in illumination of an opaque plate by laser radiation. A Melles Griot He–Ne laser of power 10 mW was used as the laser-radiation source. The speckle field produced was recorded by a CCD chamber (JAI Corp., Japan). The CCD chamber contains 768 × 494 sensitive cells located on a 6.45 × 4.84-mm matrix. In the case of the employment of this CCD chamber the time of exposure can vary from 1/60 sec to 10 μsec. The recording frequency is 25 frames per second. The signal from the CCD chamber arrives at the analog-to-digital converter (16 bits) and the graphics card of the personal computer, having a memory of 2 Mb in size. The core memory of the computer (64 Mb) is also employed. The images obtained were processed by two different methods in the regime of recording in quasireal time. In cross-correlation analysis, we calculated function (1) (its amplitude and coordinates of the maximum) from two successive frames. The computation result is output to the monitor, and the personal computer begins to process the next frames. In autocorrelation analysis, we calculate the constant of the speckle field in each subzone. The computation time is ~100

msec, which ensures the regime of quasireal time with a frequency of ~10 Hz. Examples of the results of processing of speckle fields are given in Fig. 2b–e. Figure 2b and c shows the images of the speckle fields obtained in "instantaneous" (10 μsec) and extended (1/60 sec) exposures respectively. In Fig. 2c, we clearly see the "blurring" of the speckle field, which leads to a change in its contrast, whose value, as has been noted above, is in inverse proportion to the average velocity of motion of the speckles at the analyzed point ("subzone"). Figure 2d and e shows the results of the correlation analysis. The local displacements of the speckle field that have been obtained in analysis of the distribution of (1) are shown in Fig. 2d. The computed velocity profile is linear with a satisfactory degree of accuracy, which corresponds to the model of motion selected. The velocity is measured simultaneously at 88 points ("subzones"), which provides the two-dimensional information over the entire field of flow.

A somewhat lower degree of accuracy but a much higher time resolution are ensured in the single-exposure regime (Fig. 2e). The gray intensity on the black and white scale corresponds to the contrast of the speckle field in this figure. The data given here also show a linear increase in the velocity from the center to the periphery and can be used for both quantitative measurements (with a somewhat lower degree of accuracy than in the double-exposure regime) and direct visualization of the velocity field without subsequent processing of the data obtained.

Diagnostics of Two-Phase Flows. For two-phase flows PIV diagnostics is complicated by the presence, in the flow, of a dispersed phase the size and velocity of whose particles significantly differ from the corresponding parameters of the main phase. To unambiguously evaluate the vector velocity field in the probed region of the flow we must pre-separate the phases in the PIV pictures processed. For this purpose one usually uses the digital-filtration method [21] or the mask method [22], which allow good results in the case where the particles of the dispersed and main phases significantly differ in size. In the present work, we consider the heuristic method of detection of particles and evaluation of the coordinates of their centers and the method of selection of the images of particles by their size with the use of the likelihood function [23]. The methods for solving the problem of differentiation of signals and evaluating their parameters have been developed well in mathematical statistics [24]. In the case where a priori probability densities of the values of the estimated parameters are unknown one uses the method of the maximum of the likelihood function. According to this method, differentiation of the images resulting from the scattering of laser radiation on the particles of dissimilar phases is carried out based on the computation and comparison of their likelihood functions found under different assumptions made on the size of a particle image. In so doing (unlike the mask method), one imposes smaller limitations on the size of the particle images and the number of possible discrete values of this size.

Let us consider the problem of separation (selection) of particle images for two possible values of their size. We assume that a particle image is described by one of the two models

$$u_k(x, y, R_k) = \frac{U_k}{1 + \left[\dfrac{(x - x_k)^2 + (y - y_k)^2}{R_k^2}\right]^{N_1}}, \tag{3}$$

$$u_k(x, y, R_k) = U_k \exp\left\{-\left[\frac{(x - x_k)^2 + (y - y_k)^2}{R_k^2}\right]^2\right\}, \tag{4}$$

where $u_k(x, y, R_k)$ is the intensity distribution of the image of the kth particle within a frame, U_k is the maximum level of intensity of the image of the kth particle, x_k and y_k are the coordinates of the center of the kth particle, R_k is the effective radius of the image of the kth particle, and N_1 is the parameter of intensity distribution for the first model. The parameter R_k is employed for estimation of the particle size and can take values of r_1 and r_2. The initial image is represented in the form of a matrix of discrete values of intensity. The size and range of values of the elements of this matrix are determined by the parameters of the digital CCD chamber employed for recording of PIV pictures. In developing the algorithm, we assume that additive Gaussian noise is superimposed on the image.

The procedure of separation of the phases of PIV pictures is as follows. At first we determine the coordinates of the centers of particle images and normalize their intensity levels. Thereafter, according to the criterion of the maxi-

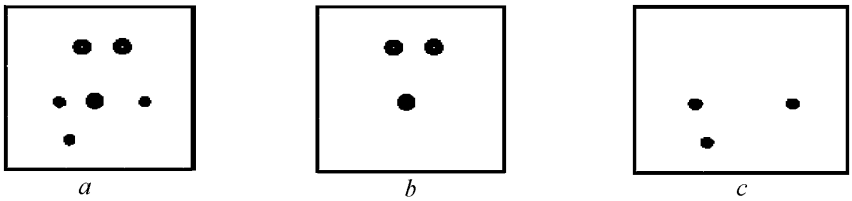

Fig. 3. Selection of particle images by size, model (1).

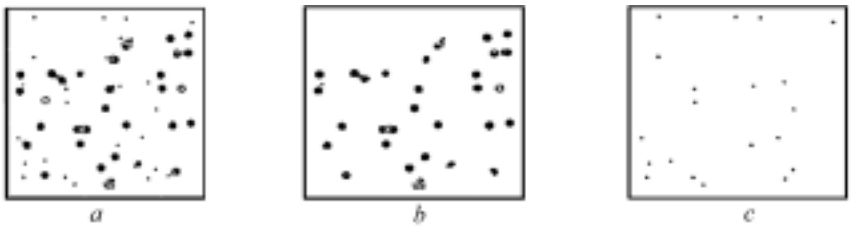

Fig. 4. Selection of particle images by size, model (2).

mum likelihood ratio, we select the particle images by their effective radii R_k. The possible values of the radii r_1 and r_2 are assumed to be known. This constraint is not fundamental, since the radius as the information parameter of the model prescribed can be evaluated in advance by the method of the maximum likelihood function. The formal algorithm for estimation of the value of the effective radius of the image of the kth particle has the form

$$R_k = \begin{cases} r_1, & \text{if} \quad q_k > 1, \\ r_2, & \text{if} \quad q_k < 1; \end{cases} \tag{5}$$

$$q_k = \frac{2 \cdot \iint\limits_S \xi(x, y)\,[u_k(x, y, r_1) - u_k(x, y, r_2)]\,dxdy}{\iint\limits_S [u_k^2(x, y, r_1) - u_k^2(x, y, r_2)]\,dxdy}, \tag{6}$$

where $\xi(x, y)$ is the matrix of the initial PIV picture, $u_k(x, y, r_1)$ is the model of the image of the kth particle with a r_1, $u_k(x, y, r_2)$ is the model of the image of the kth particle with a radius r_2, S is the region of location of the particle image in the frame processed, and x and y are the discrete values of the coordinates (in pixels) of the image elements.

Results of the Modeling of the Processing Procedure. Figures 3a and 4a show two models of the initial PIV picture of the cross section of a two-phase flow. After the procedure of digital processing described above, these pictures were subdivided into two parts. It is seen that the first part contains the images of large particles (Figs. 3b and 4b), while the second part contains the images of particles of small radius (Figs. 3c and 4c). We have also determined the coordinates of the centers of particle images. This information can be used further for calculation of the field of particle velocity in the flow. We emphasize that the method enables us to select the images not only by size but also by the parameters of shape (for example, to differentiate between spherical particles and nonspherical ones). The efficiency of the method presented has been investigated and confirmed by processing of model and real PIV pictures.

Program of Processing of PIV Pictures. Universal programs have been created at present for processing PIV pictures but they cannot be used on a mass-scale basis because of the high cost. On the other hand, standard mathematical packages, such as MathCad, MathLab, LabView, and Maple based on which one can realize specialized programs of processing of PIV pictures obtained experimentally or by modeling, are widely used.

Among the positive aspects of such an approach are:

(a) the absence of the consumption of time by programming the interface;

(b) facilitated programming in high-level algorithmic languages;

(c) simple and rapid access to the standard and nonstandard mathematical functions and the help file;

(d) the open architecture of the program for data analysis.

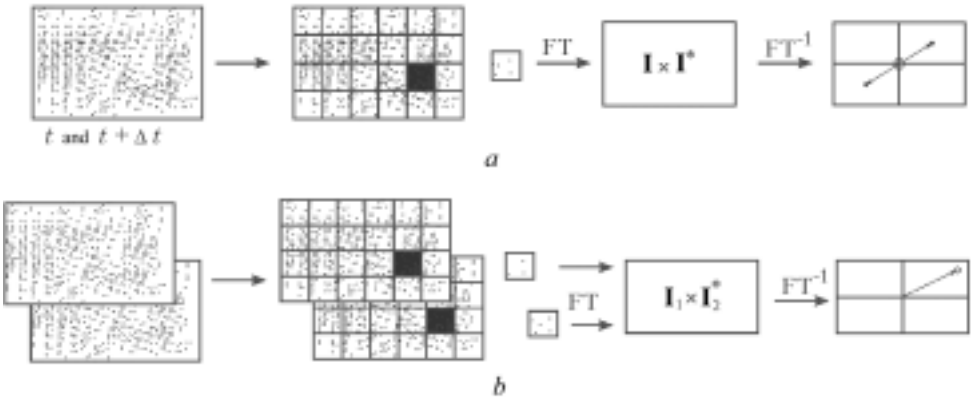

Fig. 5. Methods of processing PIV pictures: a) autocorrelation method; b) cross-correlation method (FT (FT^{-1}), direct (inverse) Fourier transformation).

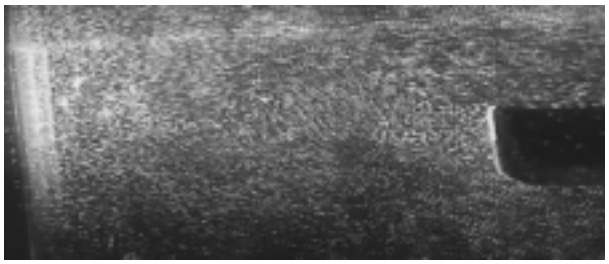

Fig. 6. Total image of two frames of the region of a two-phase flow which are taken with a time interval of Δt = 0.04 sec and the reconstructed vector velocity field.

These advantages enable the experts engaged in this field to create additional modules, to easily and rapidly re-orient the initial algorithms to a specific problem, and to use the program in the training process. The disadvantage of such an approach is the absence of a built-in graphics editor and a module for input of videoinformation flow in most of the mathematical packages, and also the much greater consumption of computer time than in the case of the programs written in low-level specialized languages.

An analysis of PIV pictures involves determination of the displacement between two images of one particle over a known period of time, which makes it possible to calculate the flow velocity (as a vector quantity) at a given point. In most cases, such problems are solved by statistical methods of auto- or cross correlation, as has been described above. When the image is broken into polling areas, they can intersect to eliminate the uncertainties at the edges and change their dimensions for a more or less detailed analysis of the features of the flow. Figure 5 shows the operational procedure for finding the auto- or cross-correlation functions with the use of a fast Fourier transformation. The program developed is written in the MathCad 2001 mathematical package and consists of a set of modules performing different operations. The program allows for the pre-filtration of images by matrix methods; it is also possible to create one's own matrix filters. To obtain a series of frames one selects the portion of interest in the videorecord and carries out frame-by-frame recording in the form of a numbered series. The images are put into the program by explicit indication of the name of files. The user can carry out pre-processing of images (filtration, enhancement of contrast and brightness). As a rule, this is used for visual detection of the images of one particle. Next, the user prescribes the dimension of the polling area N (it has an even value) and the degree of overlap of the polling areas M (it has any value from 0 to N). It takes less than 20 sec to calculate the vector field for a 756 × 256 image with N = 32 and M = 8 on a P4-1500 MHz computer. An example of the processing of a PIV record obtained in experiments with a routine videocamera is given in Fig. 6. It is noteworthy that in the program we have realized the possibility of determining the cross-correlation maximum with an error of up to tenths of a fraction of a pixel with the use of the corresponding approximation functions (there can be variants: quadratic, cubic, and Gaussian approximation functions).

Coherent Optical Processors in Systems of Dynamic Laser Anemometry. The problem of visualization of a three-dimensional spatial distribution of the velocity field in real time has not yet been satisfactorily solved. The

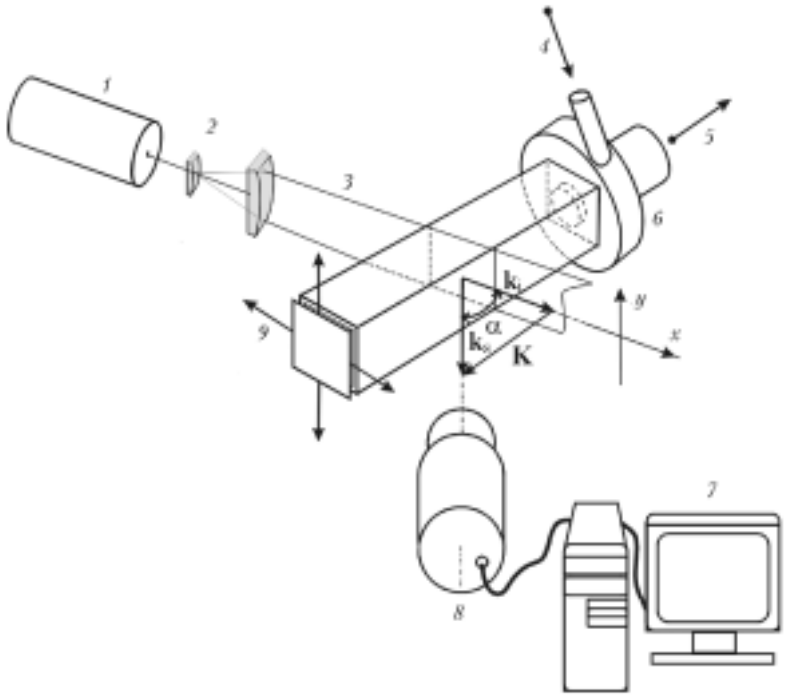

Fig. 7. Functional scheme of the experimental setup: 1) laser; 2) collimator; 3) laser knife; 4) compressed air; 5) cold air; 6) swirler; 7) personal computer; 8) optical processor; 9) hot air.

standard PIV methods have limitations related to the dependence of the measurement results on the spatial and temporal frequency of sampling and hence the concentration of visualizing particles introduced into the medium. The method of three-dimensional laser Doppler visualization and measurement in real time of the velocity field [25] which is based on the optical frequency demodulation of a light field is free of these disadvantages. The present section seeks to report the possibility of visualizing the velocity field in combined gas flows by the method proposed. Swirling (vortex) flow in a Ranque–Hilsch tube has been selected as the object of investigation. The great interest in such flows worldwide is due to the attempts at constructing an adequate physical model of energy separation in swirling flows.

A simplified diagram of the experimental unit [26] is shown in Fig. 7. The Ranque–Hilsch vortex tube represents a channel with a square cross section (34×34 mm^2) and transparent walls. Air enters the tube via a swirler. Cold air goes out through a hole at the center of the tube in the swirler plane ("cold" end of the tube). The "hot" end of the tube is manufactured in the form of a radial diffuser through which hot air goes out in radial directions. The operating regime of the tube is the same as in the measurements in [27].

The cross section under study was separated by a "laser knife." A He–Ne laser of power 15 mW operating in the principal mode was used as the source. The "laser knife" was formed in the plane orthogonal to the horizontal tube walls at an angle of $\sim 60^o$ to the tube axis. The optical axis of the processor forming the image of the flow cross section separated by the "laser knife" was oriented at an angle of $\sim 30^o$ to the "knife" plane. As follows from the geometry of light beams, correlated with the geometry of the tube, visualized was the spatial distribution of the velocity-vector component in the direction determined by the sensitivity vector **K**, which is equal to the difference of the wave vectors $\mathbf{k}_S - \mathbf{k}_i$, where $\mathbf{k}_i$ is the wave vector of radiation forming the "laser knife" and $\mathbf{k}_S$ is the wave vector of the scattered beam in the angular spectrum determined by the transmission band of the optical processor. The action of the optical processor has been described in [28]. The transfer function of the processor has a resonant form. The linear portion of the slope of the resonance amplitude-frequency characteristic of the processor is used as the discrimination curve. The mode structure of the processor is consistent with the mode structure of laser radiation. The image of the flow cross section under study is formed in the frequency-demodulated scattered light in the outlet plane of the optical processor. The intensity of the light field at each point of the image is a single-valued linear function of the projection of the velocity vector onto the direction of the sensitivity vector $\mathbf{K} = \mathbf{k}_S - \mathbf{k}_i$.

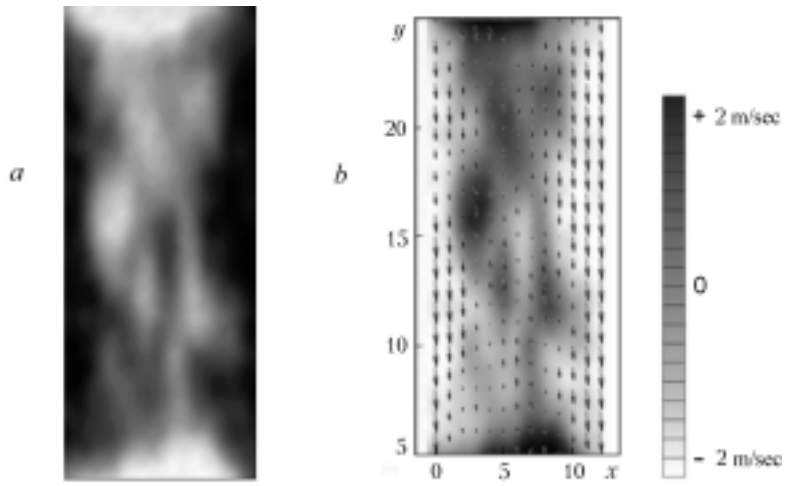

Fig. 8. Field of velocities of a swirling flow in the section adjacent to the hot end of the Ranque–Hilsch tube (a) and the reconstructed velocity distribution in the separated cross section (b). *x*, *y*, cm.

Indeed, the cross section of the medium under study illuminated by a light wave with a wave vector $\mathbf{k}_i$ is displayed at the outlet of the optical processor as the set of images of scattering optical inhomogeneities $\varphi(\xi, \eta)\delta(x - \xi, y - \eta)$, where ξ and η are the coordinates of the optical inhomogeneities in the cross-section plane (x, y). Consequently, the frequency-demodulated image of the cross section separated by the "laser knife" with a wave vector $\mathbf{k}_i$ can be described by the expression

$$\omega_D(x, y) = \gamma \int\int \mathbf{KV}(\xi, \eta)\, \varphi(\xi, \eta)\, \delta(x - \xi, y - \eta)\, d\xi d\eta = \gamma\, \mathbf{KV}(x, y)\, \varphi(x, y)\,, \tag{7}$$

where the integration is carried out over the entire separated cross section, $\omega_D(x, y)$ is the Doppler frequency shift in the light forming the point (x, y) of the image at the outlet of the optical processor, $\mathbf{V}(x, y)$ is the velocity vector at the point (x, y), and γ is the slope of the frequency discrimination characteristic of the processor. The factor $\varphi(x, y)$ corresponds to the function of scattering in the $\mathbf{k}_s$ direction, which describes the initial image of the cross-section study not subjected to frequency demodulation. Then $\tilde{\omega}_D(x, y) = \dfrac{\omega_D(x, y)}{\gamma\varphi(x, y)} = \mathbf{KV}(x, y)$ yields the distribution of the relative intensity of the frequency-demodulated image. It is seen that $\tilde{\omega}_D(x, y)$ unambiguously represents the field of the velocity component in the **K** direction:

$$|V(x, y)| = \frac{1}{K}\mathbf{V}(x, y)\,\mathbf{K}\,. \tag{8}$$

Figure 8a shows an example of the visualized velocity field [29] in the "laser-knife" plane. It is clearly seen that the velocity field contains vortex structures transformed in dynamics, including those in the form of double spirals. Figure 8b gives the reconstructured distribution in the investigated cross section of the projections of the velocity vector $\mathbf{V}(x, y)$ onto the direction of the sensitivity vector **K**. It is of interest to note that the double spirals in the field of optical phase density which were detected by the methods of Hilbert optics in 1997 [28] in the same tube in analogous flow regimes can be made to correspond to bispiral wave structures in the velocity field. Since the distribution of the phase optical density is determined by the pressure and temperature, this similarity points to the relationship of the dynamic spatial fields of pressure, temperature, and velocities in such surprising configurations observed for the first time. The method of laser Doppler visualization of the velocity vectors in the three-dimensional coordinate basis has been substantiated theoretically and experimentally in [30]. These methods represent a new trend in optical measuring techniques oriented toward use in experimental hydro- and aerodynamics and in industrial technologies related to the need for nondisturbing testing of the spatial distribution of kinematic parameters in moving media.

Real-time visualization of dynamic velocity fields makes it possible to study unsteady space-time distributions of kinematic parameters, which is a necessary condition for the creation of adequate physical models in solution of fundamental problems of hydro- and gasdynamics.

CONCLUSIONS

New PIV systems substantially extend the capabilities of laser anemometry in quantitative diagnostics and visualization of combined three-dimensional unsteady and multiphase flows. Change-over to digital technologies and direct optical processing of PIV pictures enables one to organize the monitoring of the processes investigated in real time, which opens up vast prospects for reduction of PIV systems to the practice of scientific and technological measurements.

This work was carried out under a project of the INTAS International Foundation (project No. 00-0135) and with financial support from the Ministry of Education of Russia within the framework of the program "Scientific Research of Higher School in Priority Directions of Science and Technology," project codes 208.05.01.040 and 209.01.01. 0.32, the Russian Foundation for Basic Research (projects 99-02-16702 and 00-02-17520), and the Belarusian Republic Foundation for Basic Research, project No. T02R-043. The authors express their thanks to Dr. J. Kompenhans, supervisor of the INTAS project, and Prof. W. Merzkirch for useful discussions and recommendations and to Candidates of Science in Physics and Mathematics E. I. Lavinskaya, V. A. Grechikhin, A. V. Tolkachev, P. P. Belousov, P. Ya. Belousov, and N. B. Bazylev, scientific co-workers, for their assistance in conducting the experiments and preparation of the publication.

NOTATION

C_i, constant of the speckle field in the ith subregion; d^*, linear dimension of the CCD cell, m; $\Delta\mathbf{d}$, vector of displacement of visualizing particles, m; $I_i(m, n)$, radiation intensity at the ith instant of time at the CCD-chamber cell characterized by the coordinates (m, n), W/m^2; $\mathbf{i}$, $\mathbf{j}$, and $\mathbf{k}$, unit vectors; $\mathbf{K}$, sensitivity vector, m^{-1}; $\mathbf{I}$ and $\mathbf{I}^*$, matrices; (m, n), coordinates of the cell in the CCD matrix; M and N, dimension of the CCD matrix; N_1, parameter of intensity distribution for the first model; (p, q), running coordinates of the function R; (p^*, q^*), coordinates of the maximum of the function R; r, particle size, m; R, cross-correlation function; R_k, effective radius of the image of the kth particle, m; r_1 and r_2, values of the variable R_k, m; S, region of location of the particle image in the frame processed; $\Delta\mathbf{S}$, displacement vector, m (see Fig. 1); t, time, sec; u_k, intensity distribution of the image of the kth particle within a frame, W/m^2; U_k, maximum level of intensity of the image of the kth particle, W/m^2; $\mathbf{V}$, velocity vector, m/sec; V_x, V_y, and V_z, projections of the velocity vector, m/sec; x, y, z, coordinates, m (or pixel); α, angle between the vectors $\mathbf{k}_i$ and $\mathbf{k}_s$, rad; $\xi(x, y)$, matrix of the initial PIV picture; $\varphi(\xi, \eta)$ and $\delta(x - \xi, y - \eta)$, sets of images of the scattering optical inhomogeneities; $\omega_D(x, y)$, Doppler shift of frequency, sec^{-1}; $\tilde{\omega}_D$, relative distribution of the frequency-demodulated image; $\langle ... \rangle$, average value of the quantity. Subscripts: i, incident; s, scattering.

REFERENCES

1. Yu. N. Dubnishchev and B. S. Rinkevichius, *Methods of Laser Doppler Anemometry* [in Russian], Nauka, Moscow (1982).
2. C. J. Chen and R. J. Emrich, Investigation of shock tube boundary layer by a tracer method, *Phys. Fluids*, **6**, 1–9 (1963).
3. D. B. Baker and M. E. Fourney, Measuring fluid velocities with speckle patterns, *Opt. Lett.*, **1**, 135–137 (1977).
4. T. D. Dudderar and P. G. Simpkins, Laser speckle photography in a fluid medium, *Nature*, **270**, No. 5632, 45–47 (1977).
5. R. Grousson and S. Mallick, Study of flow pattern in a fluid by scattered laser light, *Appl. Opt.*, **16**, 2334–2336 (1977).
6. N. A. Fomin, *Speckle Interferometry of Gas Flows* [in Russian], Nauka i Tekhnika, Minsk (1989).

7. R. J. Adrian, Multi-point optical measurements of simultaneous vectors in unsteady flow — A review, *Int. J. Heat Fluid Flow*, **7**, 127–145 (1986).
8. R. J. Adrian, Particle-imaging techniques for experimental fluid mechanics, *Ann. Rev. Fluid Mech.*, **23**, 261–304 (1991).
9. K. D. Hinsch, in: R. S. Sirohi (ed.), Particle Image Velocimetry (PIV), *Speckle Metrology*, Marcel Dekker, New York (1993), pp. 235–323.
10. M. Raffel, C. E. Willert, and J. Kompenhans, *Particle Image Velocimetry. A Practical Guide*, Springer-Verlag, Berlin (1998).
11. N. A. Fomin, *Speckle Photography for Fluid Mechanics Measurements*, Springer-Verlag, Berlin (1998).
12. W. Merzkirch, in: F. Mayinger and O. Feldman (eds.), *Particle Image Velocimetry. Optical Measurements — Techniques and Applications*, Ch. 16, Springer-Verlag, Berlin (2001).
13. N. B. Bazylev, S. M. Vlasenko, E. I. Lavinskaya, and N. A. Fomin, Digital speckle photography of fast processes in quasireal time, *Dokl. Nats. Akad. Nauk Belarusi*, **45**, No. 5, 55–59 (2001).
14. N. B. Bazylev, E. I. Lavinskaya, and N. A. Fomin, Influence of the processes of multiple scattering on laser probing of biotissues, *Inzh.-Fiz. Zh.*, **76**, No. 5, 16–24 (2003).
15. N. A. Fomin, U. Wernekinck, and W. Merzkirch, Speckle photography of a turbulent density field, in: M. Pichal (ed.), *Optical Methods in Dynamics of Fluids and Solids*, Springer-Verlag, Berlin (1985), pp. 159–165.
16. N. A. Fomin, C. Gray, C. Greated, et al., Turbulent flow field determination using particle image velocimetry (PIV), in: *Proc. 3rd Minsk Int. Forum "Heat and Mass Transfer–MIF-96"* [in Russian], Vol. 4, 20–24 May 1996, Minsk (1996), pp. 203–209.
17. M. P. Arroyo and C. A. Greated, Stereoscopic particle image velocimetry, *Meas. Sci. Tech.*, **2**, 1181–1186 (1991).
18. C. Brücker, 3-D PIV via spatial correlation in a color-coded light sheet, *Exp. Fluids*, **21**, 312–314 (1996).
19. D. H. Barnhart, R. J. Adrian, and G. C. Papen, Phase-conjugate holographic system for high resolution particle image velocimetry, *Appl. Opt.*, **33**, 7159–7170 (1994).
20. I. Rohle, Three-dimensional Doppler global velocimetry in the flow of a fuel spray nozzle and in the wake region of a car, *Flow Meas. Instrum.*, **7**, 287–294 (1997).
21. B. S. Rinkevichius, *Laser Diagnostics of Flow* [in Russian], Moscow (1990).
22. M. V. Yesin, B. S. Rinkevichius, and A. V. Tolkachev, Digital filtering of gas bubble images for DPIV measurements, in: *CD-ROM Proc. 4th Int. Symp. on Particle Image Velocimetry*, Paper No. 1091, Gottingen, Germany, 2001.
23. L. Gui and W. Merzkirch, Phase-separation of PIV measurements in two-phase flow by applying a digital mask technique, *ERCOFTAC Bull.*, **30**, 45–48 (1996).
24. H. Cramer, *Mathematical Methods of Statistics* [Russian translation], Mir, Moscow (1975).
25. Yu. N. Dubnishchev, Advanced optical methods for diagnostics of flow. Laser metrology applied to science, industry and everyday life, *Proc. SPIE*, **4900**, 1130–1139 (2002).
26. P. P. Belousov, P. Ya. Belousov, and Yu. N. Dubnishchev, Laser Doppler visualization of the velocity field, *Quant. Electron.*, **29**, No. 11, 995–1000 (1999).
27. V. A. Arbuzov, Yu. N. Dubnishchev, A. V. Lebedev, et al., Observation of large-scale hydrodynamic structures in the vortex tube and the Ranque effect, *Pis'ma Zh. Tekh. Fiz.*, **23**, No. 23, 84–90 (1997).
28. P. P. Belousov, P. Ya. Belousov, and Yu. N. Dubnishchev, Laser Doppler visualization of the velocity field in the Ranque vortex flow, *Pis'ma Zh. Tekh. Fiz.*, **28**, No. 16, 6–11 (2002).
29. P. P. Belousov, P. Ya. Belousov, and Yu. N. Dubnishchev, Laser Doppler visualization of the velocity field in the Ranque vortex flow, in: *Proc. 10th Int. Symp. on Flow Visualization*, Paper No. F0353, 26–29 August, 2002, Kyoto, Japan (2000).
30. P. P. Belousov, P. Ya. Belousov, and Yu. N. Dubnishchev, Laser Doppler visualization of 3D velocity flow, *Optoelectron., Instrum. Data Process.*, **5**, 1–8 (2001).